Reverse Engineering the Dynamics of Human Pursuit Strategies

Undergraduate Honors Thesis

Presented in Partial Fulfillment of the Requirements for Graduation
with Honors Research Distinction
in the Department of Mechanical and Aerospace Engineering
at The Ohio State University

By:
Dheepak Arumukhom Revi

Thesis Committee:
Professor Manoj Srinivasan (Advisor)
Professor Sandra Metzler

November 2016

Abstract

Many animals in the wild often perform pursuit and evasion in order to survive – pursuing prey or evading predators. In modern humans, such pursuit and evasion are most often seen in various sports and children's games. Here, we examine what pursuit strategies people use to catch an evader, as in a game of tag. We performed human subject experiments in which we tested pursuit-evasion scenarios with two subjects per trial, one the pursuer and the other the evader, and eleven subject pairs. We used multiple protocols, with differing evader motion – evader moving in a straight line, a circle, or free-form, and the evader being able to change direction or not (when moving in a straight line or circle). Pursuer and evader motion data were obtained using stereogrammetry techniques with three cameras. We compared the data with a few mathematical model of pursuit, including pure pursuit, lead, and lag pursuit, proportional navigation. We also fit the pursuer velocity data to linear models of evader variables. While the median strategy used by the pursuers was close to pure pursuit, we found that pursuers used a lead strategy when the evader was more constrained and therefore more predictable – for instance, when the evader moved in a straight line without changing direction. We also found that on average 40% of the pursuers motion variance (velocity magnitude and direction) can be explained by using simple models, relating to evader motion (velocity magnitude and direction) and the distance between the pursuer and evader.

Acknowledgments

I would like to first acknowledge my parents for their ever ending supporting in my career decisions. Without the both of them, I would have never been able to come to the USA in the first place, let alone be accepted into a great university like The Ohio State University. All my accomplishments thus far in life has some kind of direct correlation with my parents' support. So from the bottom of my heart, I thank my parents for their continued support.

I would think to thank my advisor Dr. Manoj Srinivasan for always being there for me, and helping me through my problem, both academically and non-academically. I am truly grateful to have a mentor as passionate and motivating like him. You elevated my passion in research, by allowing me to explore my own methods, while constantly challenging me to raise my bar. My only regret is not being able to take a formal class with him, but I have learned and continue to learn a lot from him as an example. So once again thank you, Dr. Srinivasan, for helping me start a career.

I would like to thank all my friends and lab mates for your constant support in this project. Thanks to my lab mates (especially Varun Joshi, Nidhi Seethapathi, and Kevin Lehtinen) for helping me in various aspects and giving me a fresh angle whenever I approached them when a problem. Thanks also to Dr. Sandra Metzler for being on my thesis committee and for thoughtful comments on the thesis.

Lastly, I would like to thank my high school robotics mentor Mr. Greg King for this inspiration and guidance he provided in high school. Without his unbound inspiration and trust placed in me, I would have never picked mechanical engineering as my major, nor would I have been so excited to learn engineering and robotics.

Table of Contents

List of Tables

List of Figures

Chapter 1: Introduction

1.1 Motivation

Pursuit and evasion are behavioral traits in many animals. Animals are often trying to get away from predators or get to some preys. Thus, good pursuit and evasion performance may improve the animal's likelihood of survival in the wild. Figure 1.1 shows a cheetah in pursuit of a rabbit. While most modern humans do not explicitly have to hunt or evade predators, it may be that pursuit and evasion strategies that were invaluable during our evolutionary past and may still be inherent in guiding our dynamics. For instance, modern humans may use evasion strategies to successfully move around on a crowded street with bumping into their neighbor. Humans use pursuit and evasion strategies in various sports, e.g., football, soccer, hockey, etc. Even sports played in smaller arenas like tennis requires interception of the ball, which has similarities to pursuit tasks. The obvious example of pursuit and evasion strategies in sports is the *game of tag* played by children, shown in Figure 1.2. The question here is how do humans do these activities? Why do we take the path we do? What is the controller that our brain uses in order to successfully capture a target or evade a pursuer? Can we characterize these motions into a mathematical equation that can be used to predict human pursuit and evasion? And finally, are humans choosing a time-optimal strategy for successful pursuit and evasion? Here, we perform human subject experiments and mathematical modeling towards answering some of these questions.

Figure 1.1: Cheetah pursuing an evading rabbit. Photo credit: David Nunn, https://www.flickr.com/photos/davidnunn/ CC BY-NC-ND 2.0.

Figure 1.2: A child chasing an adult in a game of tag. Photo credit: U.S. Navy photo by Mass Communications Specialist 1st Class Johnie Hickmon [Public domain], via Wikimedia Commons.

1.2 Purpose of Research

The objectives of this study are to:

1) Observe and characterize strategies used by humans in pursuing an evading target with different constraints on their movement and initial conditions.
2) Create a mathematical model of the pursuer motion that is able to accurately predict similar motion and validate it using experimental results.

1.3 Significance of Research

Why study pursuit? The mathematical complexity of pursuit (not particular to humans) has been studied by many people throughout the past, as early as 2000 B.C (Nahin 2012). Understanding the behavioral dynamics of pursuit or evasion can be used in a wide range of applications, from sports planning, to missile guidance control. We can use pursuit strategies to predict the path that a player may take in sports such as soccer or football, and can potentially recommend an optimal path for amateur players to play the sport more successfully. Understanding pursuit and evasion strategies may allow the design of more realistic computer games and animation movies. Optimal pursuit and evasion strategies could be used by disaster relief robots and autonomous cars to effectively path plan, especially since both applications have an uncharacterized human component that adds on to its existing path planning dynamics. For instance, we could use these strategies to help the robot get to its target faster or assist the car in avoiding hitting a walking pedestrians or deer. The strategies derived may also be helpful in guiding a missile toward another evading missile.

Much more broadly, understanding how humans move and react in a variety of situations can perhaps be used in designing tools for humans, from better shoes to better prosthetic devices. Understanding the pursuit and evasion strategies used by humans may also provide unique insight into the evolutionary past of humankind.

1.4 Literature Review

1.4.1 Existing Literature on Human Biomechanics

When required to move from point A to another point B, humans use either a "walking" or a "running" gait. Walking, in general, is used at a lower speed and running at higher speed. Why do humans commonly exhibit this particular gait at their respective speeds? Energy optimization, which states that humans move in a manner that minimizes the metabolic energy of their motion (Ralston 1958, Srinivasan 2009, Long and Srinivasan 2013) is thought to be a possible solution to this problem. Although running in an absolute sense uses more metabolic energy than walking, experimental evidence shows that metabolic energy cost of walking was lower than that of running at low speeds and higher at higher speeds (Alexander 1976, 1989, 2003, Hoyt & Taylor 1981). While energy optimality is a good predictor of slow-speed steady state locomotion, we do not know if this principle will apply to pursuit and evasion tasks.

1.4.2 Existing Pursuit Strategies

Military airplanes and missile have long been using intercepting (pursuit) and maneuvering (evasion) strategies on the battlefield. In their case, a successful pursuit means the plane or missile was able to neutralize the threat, and successful evasion means the plane was able to escape the threat. In terms of pursuit, most pilots are taught some basic maneuvers to intercept a

moving target. The three most common types of pursuit maneuver a pilot can do to catch a target are: pure pursuit, lead pursuit and lag pursuit (SimHQ 1998).

Pure Pursuit: is when the velocity vector of the pursuer is always directly aligned towards the evader's velocity vector (Nahin 2012, SimHQ 1998). See Figure 1.3.

Lead Pursuit: is when the velocity vector of the pursuer is always aligned directly ahead of the evader's velocity vector (SimHQ 1998). See Figure 1.3.

Lag Pursuit: is when the velocity vector of the pursuer is always aligned directly behind the evader's velocity vector (SimHQ 1998). See Figure 1.3.

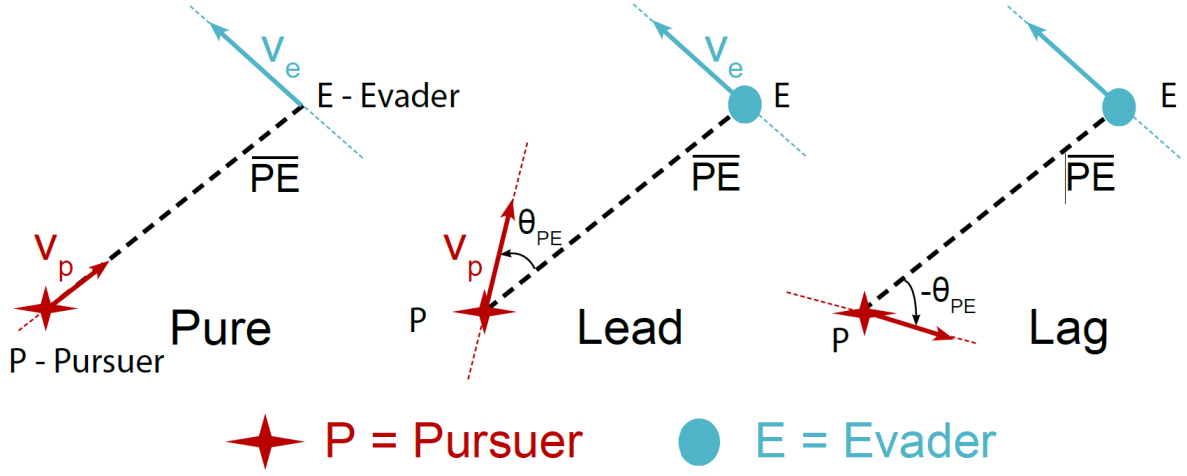

Figure 1.3: Pure, Lead, and Lag Pursuit Strategies

For a homing missile i.e. a missile with active sensing and target tracking, the pursuit strategies most commonly used is the proportional navigation strategy (Ghose 2012). The mechanism of this strategy depends on several factors, including types of inertial and target sensing available and the line of sight (PE vector) reconstruction process (Palumbo 2010). In general, there are four types of proportional navigation strategies: pure proportional navigation, true proportional navigation, generalized true proportional navigation and ideal proportional navigation. For true

proportional navigation the pursuer acceleration (a_p) is normal to vector PE and is made proportional to the rotation rate of the vector PE ($\dot{\theta}_{PE}$) and the closing speed (V_p) (Ghose 2012). See Figure 1.4.

$$a_p = N' V_p \dot{\theta}_{PE} \qquad \text{(Equation 1)}$$

Proportional navigation has a few variants, all of which have a similar form in that they are still proportional to the rotation rate of the vector PE, but the details of the pursuer velocity direction are different. In "true proportional navigation" (figure 1.4), the pursuer acceleration ($\boldsymbol{a_p}$) is applied perpendicular to the line joining the pursuer and evader ($\boldsymbol{PE}$). In "pure proportional navigation" (figure 1.5a), the pursuer acceleration ($\boldsymbol{a_p}$) is normal to the pursuer velocity ($\boldsymbol{V_p}$). In "generalized true proportional navigation" (figure 1.5b), the pursuer has the freedom of choosing the direction ($\boldsymbol{\eta}$) lateral acceleration, but for the complexity of its controller, the performance is not justified (Ghose 2012). In "ideal proportional navigation" (figure 1.5c), the lateral acceleration is applied perpendicular to the relative velocity ($\boldsymbol{V_R}$) between pursuer and evader (Ghose 2012).

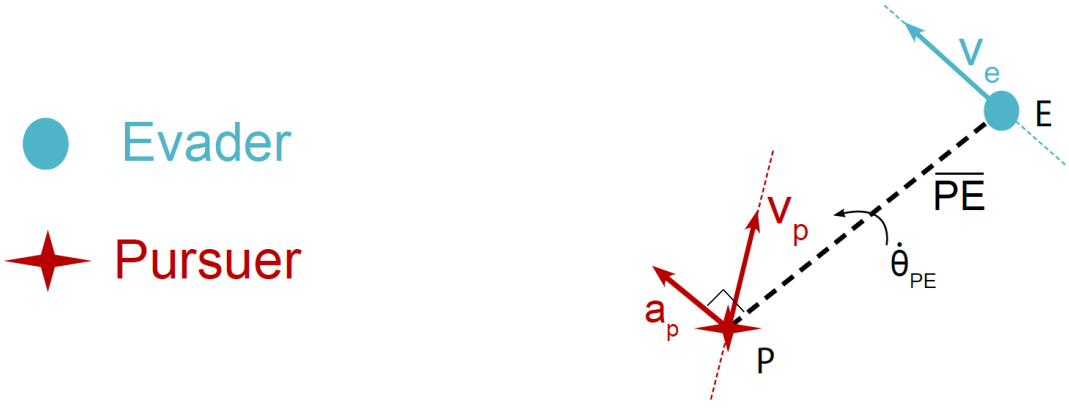

Figure 1.4: True Proportional Navigation Strategy

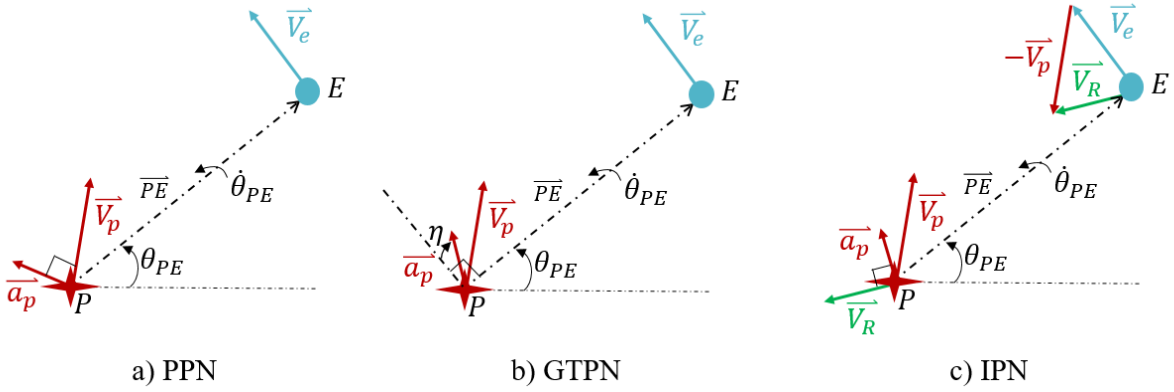

a) PPN b) GTPN c) IPN

Figure 1.5: Variants of Proportional Navigation Strategies: PPN – Pure Proportional Navigation; GTPN – Generalized Proportional Navigation and IPN – Ideal Proportional Navigation

Another strategy used by the pursuer has a similar flavor as a football player "mirroring" another football players motion. Here, the tackler "mirrors" the runner's path, while also moving forward toward the evader. This strategy works when there is an established boundary and it ensures that the runner is caught independent of the path the runner takes (Connell 1995). This mirroring strategy is less useful when the evader is unbounded by established boundaries.

Chapter 2: Methodology

This chapter outlines the experimental procedures and protocols we used to characterize pursuit and evasion. The processing of the experimental data required to get the position vectors of pursuer and evader as a function of time is also discussed below.

2.1 Experiment outline in brief

We developed and tested five pursuit-evasion protocols. Each pursuit-evasion scenario required two subjects, one as the pursuer and the other as evader for the experiment. The two human subjects are considered to be "one subject pair" for the experiment. We tested eleven such subject pairs. A basic visual inspection is used to identify which subject is faster by making both subjects run across the room. The faster subject is assigned to be the pursuer and the slower one is assigned to be the evader. The pursuer and evader are then given different spatial and trajectory constraints in accordance with its respective protocol. In general, the pursuer is always asked to catch the evader as fast as possible and the evader is always asked to avoid capture for as long as possible, both within the given constraints by their respective protocols. When capture happens, that trial is considered to be complete and the subject pair starts the next trial. There are five protocols in total, with multiple trials within each protocol.

2.2 Subject Population

Eleven subject pairs (22 subjects) completed this experiment (7 male pairs and 4 female pairs) with age ranging between 20 and 25. The average height of the subject was 1.741 ± 0.104 m, and the average mass of the person was 71.068 ± 13.407 kg. Data for two out of the eleven subject pairs was not processed due to the bad lighting in the room. (Refer Appendix A for data processing methods). All subjects participated with an informed consent about their role in this experiment. The protocols were approved by The Ohio State University Institutional Review Board.

Criteria for Inclusion: Healthy adults of either sex who ages lie between 18 and 35, and are able to move, walk and run at moderate speeds are considered for this experiment.
Criteria for Exclusion: People who are not able to walk or run at moderate speed independently, pregnant, having a history of heart or lung problems, or other movement disorders are not considered for this experiment.

Choosing Pursuer and Evader: The faster subject is generally assigned to be the pursuer and the slower subject is assigned to be the evader. Since every trial ends after the capture, this is done simply to avoid a scenario where the evader is too fast to be caught and the trials don't end. Thus, the evader is intentionally set up to fail, as we want to study the pursuer motion in detail and do not analyze the evader as much. The pursuer and the evader were always of the same gender.

2.3 Setup and Instrumentation

The experiment was conducted in a closed room with approximately 6.5 m x 11.5 m to run. The experimental room setup is shown in figure 2.1. Three cameras were mounted on the three corners of the room, capturing the entire event. The subjects were each given a different color hat, with pursuer wearing an orange hat and the evader wearing a blue or yellow hat. Both subjects are also given an internal measurement unit (IMU) to track their acceleration and orientation during the experiment. The cameras are used to track the hats and interpolate spatial information ([x y z] coordinates) about the subjects by using Euclidian geometry and transformation matrix (refer to Section 2.5). For calibrating these cameras, a calibration rod with known height was placed in seven known locations in the room. The cameras use 14 points to accurately calibrate and reconstruct the positional data with an error of less than 8cm. The operating frequency of the camera (video) and the IMU are 30 Hz and 10 Hz respectively. The spatial recreation to positional data [x y z] is included in Appendix A.

Before starting the experiment, all subjects are measured for their height, weight, arm length, and arm span as illustrated in Figure 2.2. Additionally, the average speed of each subject is also collected by asking the subject to run from one corner of the room to the other (about 14m) and recording the time it takes for the subject to get to the other corner. This metric is used to pick the role of each subject in this experiment.

Figure 2.1: Experimental Room Setup from One of the Cameras

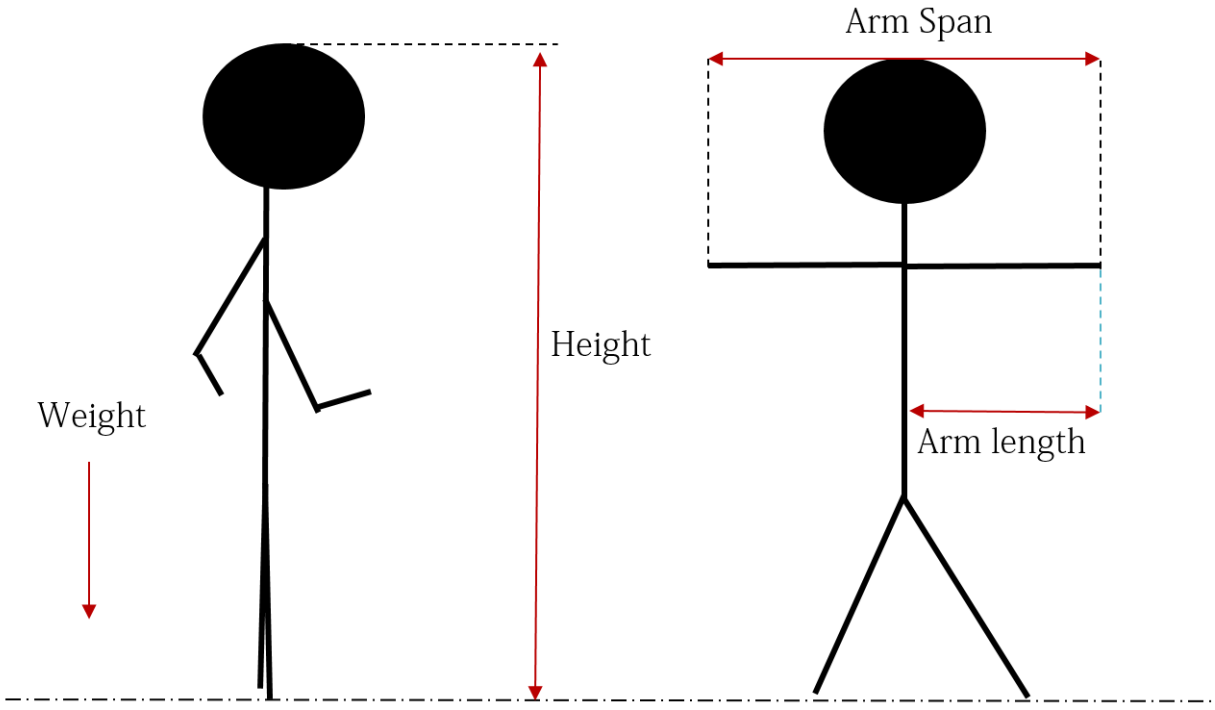

Figure 2.2: Anthropometric Data collected for each subject

2.4 Protocols

Total of five protocols were developed to constrain the pursuer and evader in different ways and study the kinds of strategies used by the pursuer in each case, described in greater detail below (see figure 2.1).

2.4.1 Protocol 1: Straight Line Uni-Directional Evader Motion

In protocol 1, the evader is constrained to running on a straight line 11.5 m long along the y-axis, marked up by chalk. The evader is asked to start the evasion from one of the three starting conditions along the line at 0m, 1.25m or 2.5m from the x-axis. The evader is only allowed to move forward along this line from where ever he/she starts and cannot change direction. The pursuer is asked to start the pursuit from one of five starting conditions constrained along the x-axis at 1.25m, 2.5m, 3.75m, 5m, and 6.25m. The evader is asked to avoid the pursuer as long as possible, within the stated constraints. The pursuer is allowed to take whatever path in order to catch the evader as fast as possible. See Figure 2.3 for an illustration of the protocol initial conditions. There are 15 unique trials (starting conditions) in this protocol, with different starting conditions for pursuer and evader. Each unique trial was repeated two times in total with the same subject pair, giving 30 trials for this protocol 1.

2.4.2 Protocol 2: Straight Line Bi-Directional Evader Motion

In protocol 2, the evader is still constrained along a line as in protocol 1, but the important difference is that, in protocol 2, the evader is allowed to switch direction (move forward and backward). For instance, the evader can first travel along the line for 5m forwards and then turn back and travel back to the start. To encourage switching direction, the starting condition of the

evader and pursuer is moved to the center of the room. That is, the x-axis is shifted by 5.75m along the y-axis compared to protocol 1. Look at figure 2.3 for a visual representation of this condition. In total, there are 30 trials within protocol 2, for the same reasons as protocol 1.

2.4.3 Protocol 3: Free Form Evader Motion

In protocol 3, the pursuer and evader are least constrained. Both the pursuer and the evader are asked to start at two adjacent corners of the room and begin the trial. The pursuer is asked to catch the evader as fast as possible and the evader to avoid the pursuer as long as possible. The path both pursuer and evader take to accomplish this is left up to each individual and the experiment is concluded when capture happens. Due to the countless variation in the path, both pursuer and evader can take for this trial, this trial is repeated 10 times.

2.4.4 Protocol 4: Circular Uni-Directional Evader Motion

In protocol 4, the evader is constrained to evade along the circumference of a circle (D = 6.5m). In the protocol the evader has the option to choose if he/she want to go around the circle in a clockwise or counterclockwise manner; but once he/she picks a direction, he/she cannot change the direction for that particular trial. The pursuer is allowed to take any path to minimize the time to capture. The only constraint the pursuer must follow is the initial starting conditions. There are eight different starting condition for the pursuer, as highlighted in figure 2.3. We had two trials per starting condition, giving a total of 16 trials with this protocol.

2.4.5 Protocol 5: Circular Bi-Directional Evader Motion

In protocol 5, the pursuer and the evader are still constrained like protocol 4, but the important difference is that, in protocol 5, the evader is allowed to switch direction from clockwise to counterclockwise or vice versa at any point in the trial. For instance, the evader can first choose to travel clockwise along the circle and then can change to counterclockwise at any point if he/she thinks that changing direction can avoid capture. In total, there are 16 trials within protocol 5, for the same reasons as protocol 4.

During all of these protocols, the trial order was randomly picked using a Matlab code. Between two protocols, the subjects were given mandatory rest of at least 5 mins. The subjects could also ask for rest whenever they feel fatigued. The subject could also discontinue the experiment at any time during the experiment. In total each subject pair performed 102 or fewer trials. Table 2.1 lists the mean and standard deviation of the number of trials per subject pair and the time duration of trials for each protocol.

Table 2.1: Statistical Information about the Experiment

	Mean Number of Trials	Std. Deviation of Number of Trials	Mean Duration of Trial	Std. Deviation of Duration of Trial
Protocol 1	22	13	2.578 sec	0.877 sec
Protocol 2	26	10	2.221 sec	0.864 sec
Protocol 3	9	2	4.256 sec	2.538 sec
Protocol 4	10	8	2.037 sec	1.069 sec
Protocol 5	10	8	2.609 sec	1.832 sec
Overall	78	34	2.593 sec	1.221 sec

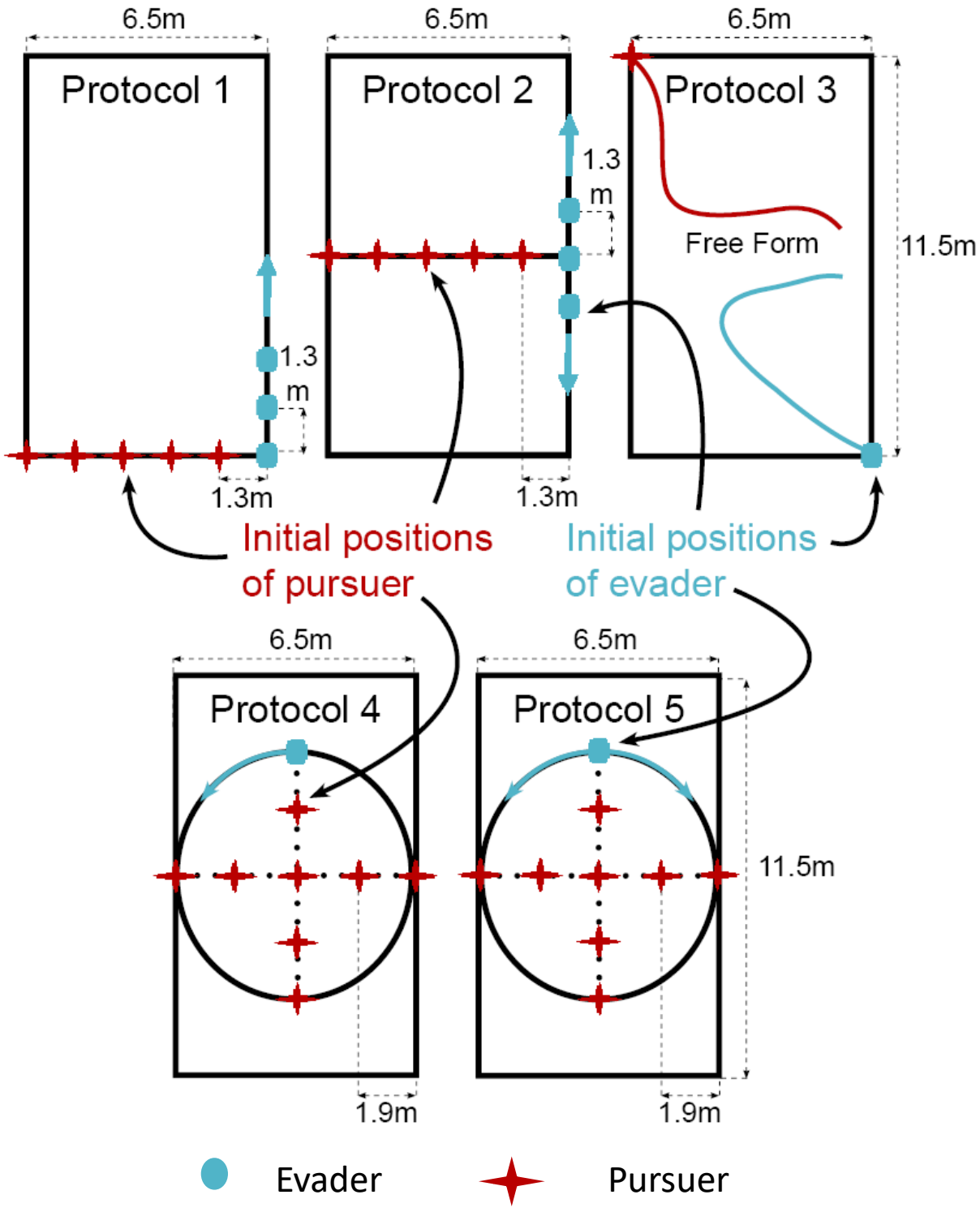

Figure 2.3: Setup for different protocols: (a) Protocol 1: Straight line uni-directional evader motion (b) Protocol 2: Straight line bi-directional evader motion (c) Protocol 3: Freeform evader motion (d) Protocol 4: Circular uni-directional evader motion (e) Protocol 5: Circular bi-directional evader motion

2.5 Data Processing

Three video cameras and Inertial Measurement Unit (IMU) sensors are used to collect visual, acceleration, and orientation data. The cameras are first synchronized to ensure that all cameras are capturing at the same event at a time instance. For this, sounds different to the background noise were produced every 10-15 minutes during the experiment. Then, the three video files were synced using the soundtracks, using the software Cyber Link Power Director.

The IMU data was not utilized for this analysis, but if we ever intend to use the IMU data, then we need to synchronize the IMU data and the camera data. For this, we proposed to do two things: one is to drop the IMU and clap when the IMU lands on the floor. The IMU would register a huge acceleration (due to impulse) and the cameras would register a spike in sound. This event could be processed and can be used to sync the IMU data to the camera data. Another way to sync is to look at the raw acceleration data the IMU registers and compare it to the second derivative of the position vector obtained using the camera. This method could potentially be noisy but ultimately be used to sync the IMU to the camera.

We manually decide the starting and the ending frames of each trail and process all frames between these from all three videos. We use the color of the hats to find the [x,y] position of the hats in each image. Figure 2.4 illustrates the process. From the [x,y] of the hats in each image, we use the knowledge of the cameras location to give us 3-D positions of the two subjects to within ±0.2m accuracy in a relevant plane (refer to Appendix A). The 3D position can be used to test different models associated with pursuit and evasion. Refer to Figure 2.5.

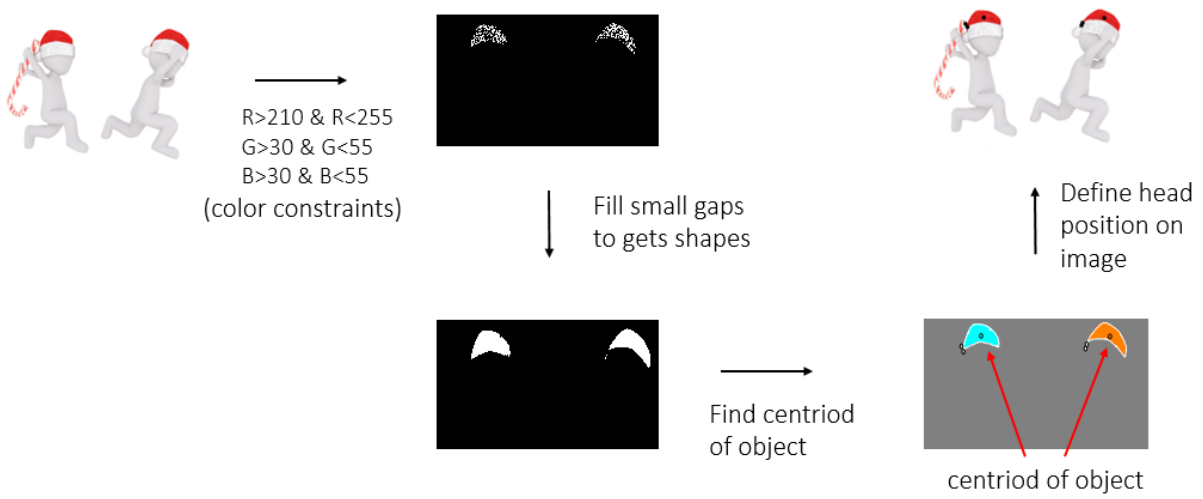

Figure 2.4: Image Processing Flow Chart: Going from color images to centroids of the hats worn by the two subjects.

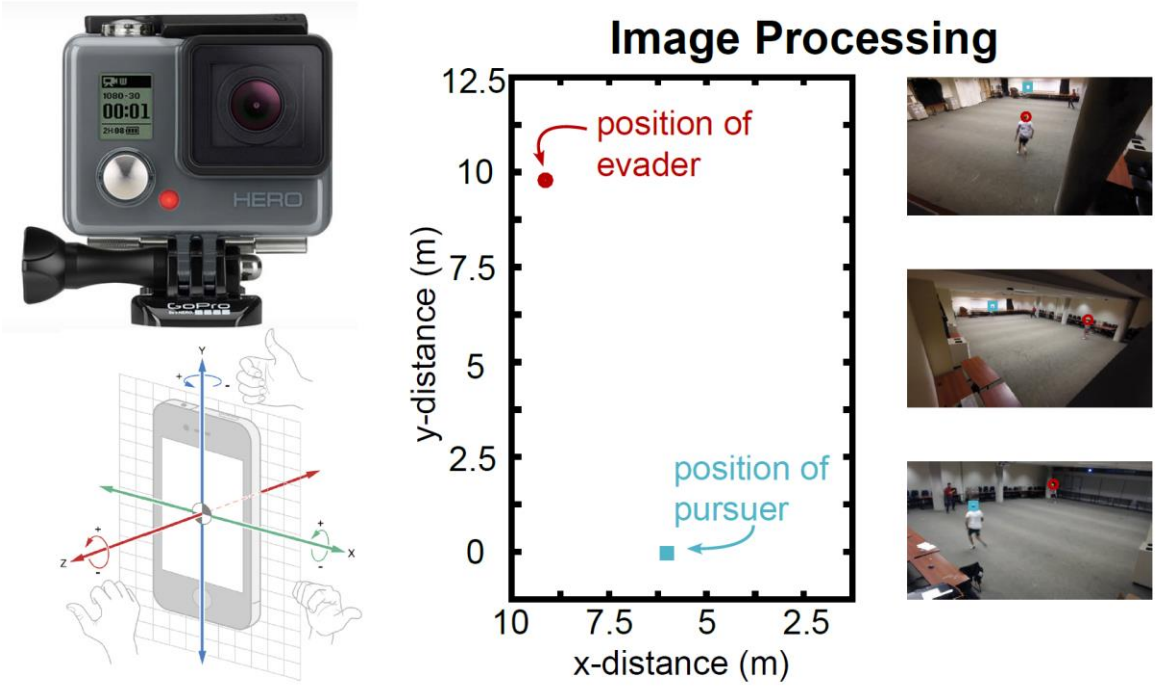

Figure 2.5: a) Instrumentation: Camera and mobile phone with IMU. b) Three camera Views to 3D point in the World.

Chapter 3: Results and Discussion

3.1 Analysis of Simple Pursuit

If we imagine that the pursuer is performing either pure, lead or lag pursuit, we can then examine which strategy is used by examining angle θ_{PE} between the pursuer velocity vector and PE vector (refer to Equation 2 and figure 3.1). Equivalent information is contained in the dot product of unit vectors along pursuer velocity and PE. For this analysis, if the theta angle is zero or if the dot product is unity (one), the pursuer is in "pure pursuit." If the theta angle is negative, then the pursuer is in lag pursuit and if the theta angle is positive, then the pursuer is in lead pursuit. Similarly, if the dot product of unit vectors along pursuer velocity and PE is close to one then, the pursuer is said to be in pure pursuit. If the dot product is less than one, than the pursuer is either in lag or lead.

$$\theta_{PE} = \sin^{-1}\left(\frac{\overline{PE}\times\bar{V}_p}{|PE||V_p|}\right)\left(\frac{V_p \cdot V_e}{|V_p||V_e|}\right) \qquad \text{(Equation 2)}$$

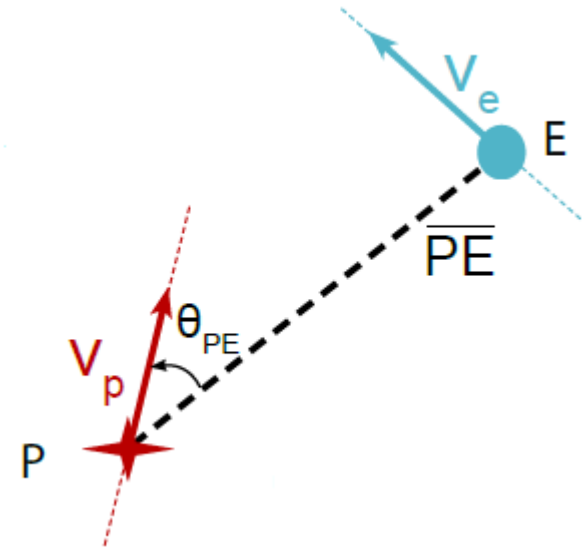

Figure 3.1: Pure, Lead, and Lag Pursuit Model

Table 3.1 reports the median and standard deviation theta values for a particular protocol across all respective trails and subject pairs. The median theta value at the beginning of the trial ("theta start", first five points) and the end of the trial ("theta end", last five points) are also reported to see the progression of theta across each protocol. The mean, median and standard deviation of the dot product between pursuer velocity vector and the relative distance vector is also reported. Additionally, the pursuer speed in each protocol is plotted against the evader speed, and the slope and intercepts of a linear fit are also noted (Figures 3.2 and 3.4).

Table 3.1: Checking for Pure, Lead, and Lag Pursuit

	Protocol 1	Protocol 2	Protocol 3	Protocol 4	Protocol 5
Theta Median	25.2819	8.6157	-3.0105	21.9848	18.9774
Theta Standard Deviation	25.4814	20.9130	23.0572	26.7257	28.2815
Theta Start	31.0187	-7.4047	-8.7222	2.4371	-0.4931
Theta End	18.1763	8.4803	6.5340	11.1019	12.330
$\overrightarrow{V_p} \cdot \overrightarrow{PE}$ Mean	0.8014	0.9033	0.9051	0.8141	0.8260
$\overrightarrow{V_p} \cdot \overrightarrow{PE}$ Median	0.8845	0.9721	0.9830	0.8973	0.9115
$\overrightarrow{V_p} \cdot \overrightarrow{PE}$ Standard Deviation	0.2311	0.1974	0.2276	0.2473	0.2344
Ve vs Vp Slope	0.7205	0.4269	0.2044	0.4179	0.3441
Ve vs Vp Intercept	1.542	1.955	2.443	1.529	1.713

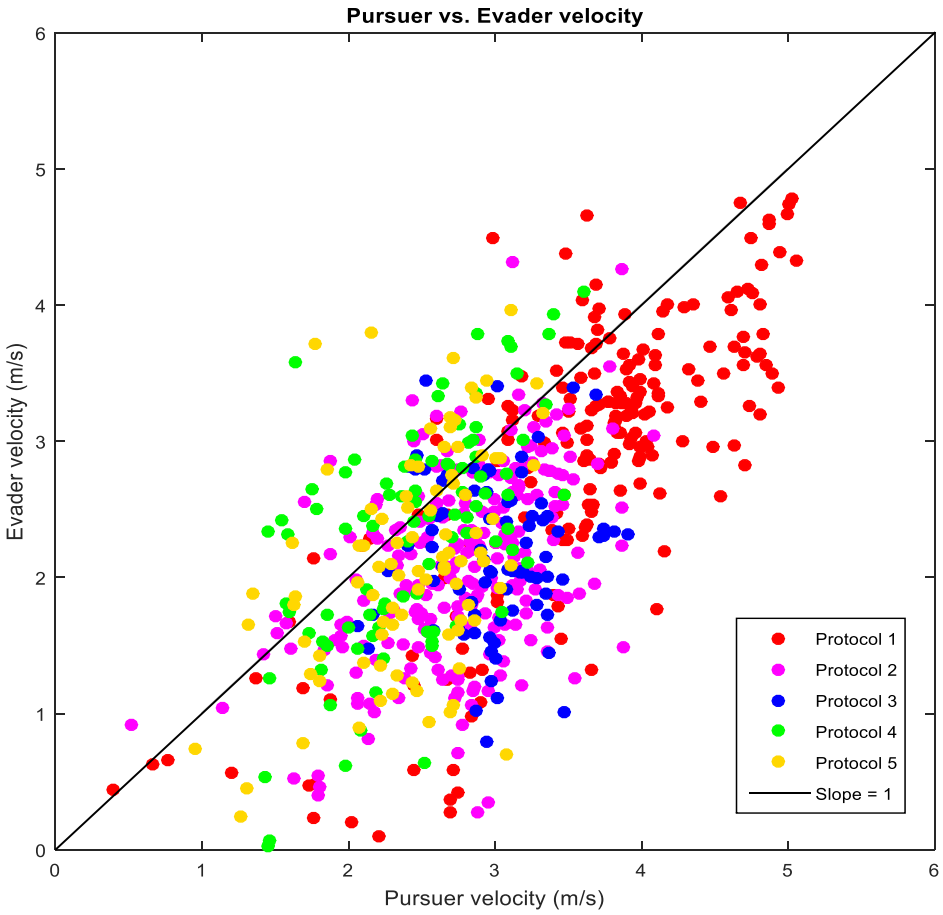

Figure 3.2: Pursuer speed vs. Evader speed for different protocols

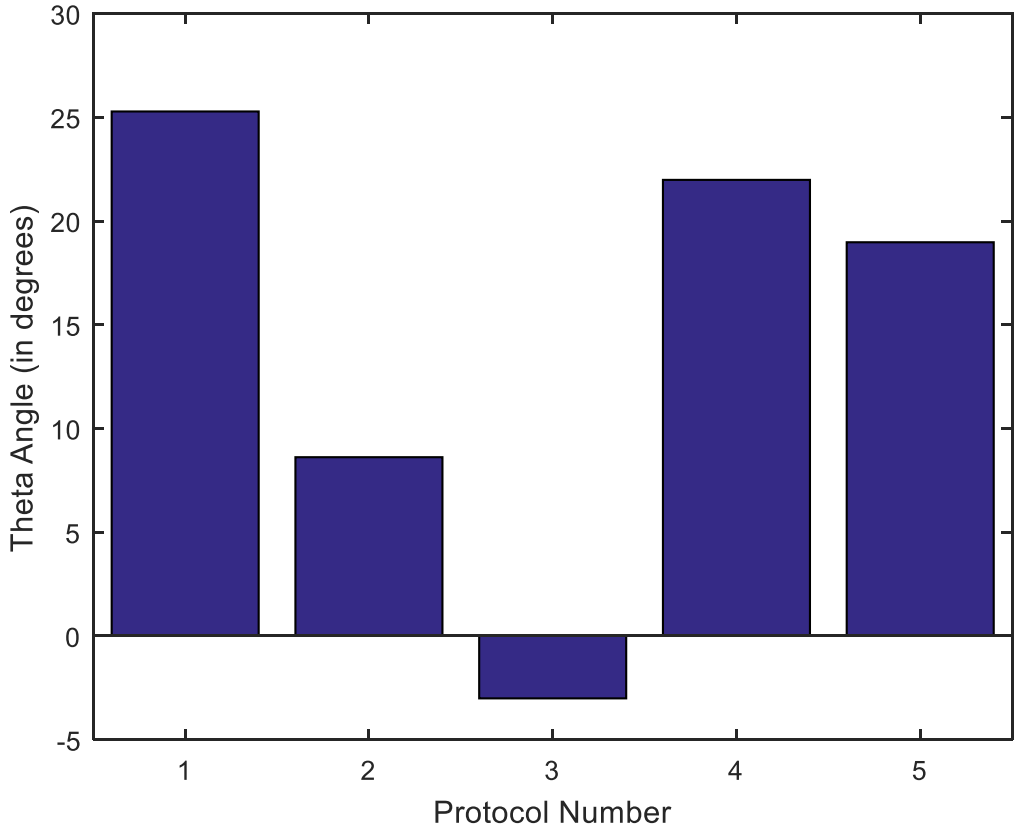

Figure 3.3: Mean theta angle across all subject pairs for the different protocols

From Table 3.1 and Figure 3.3, we see that as we decrease the constraints applied on the evader, i.e. from being bound to a line (P1, P2) or circle (P4, P5) to freeform (P3) the median theta value decreases. This means that if you constrain the evader, the pursuer will choose a lead strategy. Likewise, if the evader is not constrained and therefore less predictable, the pursuer will choose a lag strategy. This behavior makes intuitive sense because the pursuer can easily predict the evader's path in a constrained setting and thus with the lead strategy can catch the evader faster than not predicting the evaders path. Likewise, when the pursuer cannot predict the evader's path, using a lead pursuit wouldn't be helpful. Imagine a situation when the evader performs swift direction change, predicting or extrapolating the path too far into the future. In this case, a

lead strategy can actually waste time. Also, the slight lag that is seen in protocol 3 may just be an artifact of the reaction time the pursuer needs to correct his/her trajectory.

Table 3.1 also shows the mean and median dot product of pursuer velocity along the relative distance between pursuer and evader. As the constraints on the evader decrease, the unit vector approaches 1; which means that V_p vector would be along the direction of PE vector. This would further inform that the pursuer is decreasing the degree of lead as you decrease the constraints on the evader.

It appears from figure 3.3 that the evader running in a circle results in a pursuit controller that is between the controllers used when the evader uni-directionally and bi-directionally on a straight line.

Another interesting observation can be seen when the magnitude of the pursuer velocity is plotted against the magnitude of the evader velocity and the linear fit of this graph is explored (Figure 3.2).

$$V_p = mV_e + b$$

The slopes *m* and intercepts *b* for this best linear fit is visualized in Figure 3.4. The slope coefficient (*m*) decreases, as you decrease the constraints on the evader. This mean that the pursuer speed of pursuit on average is also related to the constraints placed on the evader and further as the constraints on the evader increases, the pursuers reliance on evaders speed increases. The intercept coefficient (*b*) increases, as you decrease the constraints on the evader.

This means that pursuers have some kind of generic offset based on the constraints placed on the evader. Further, this constraint increases with decreasing constraints on the evader.

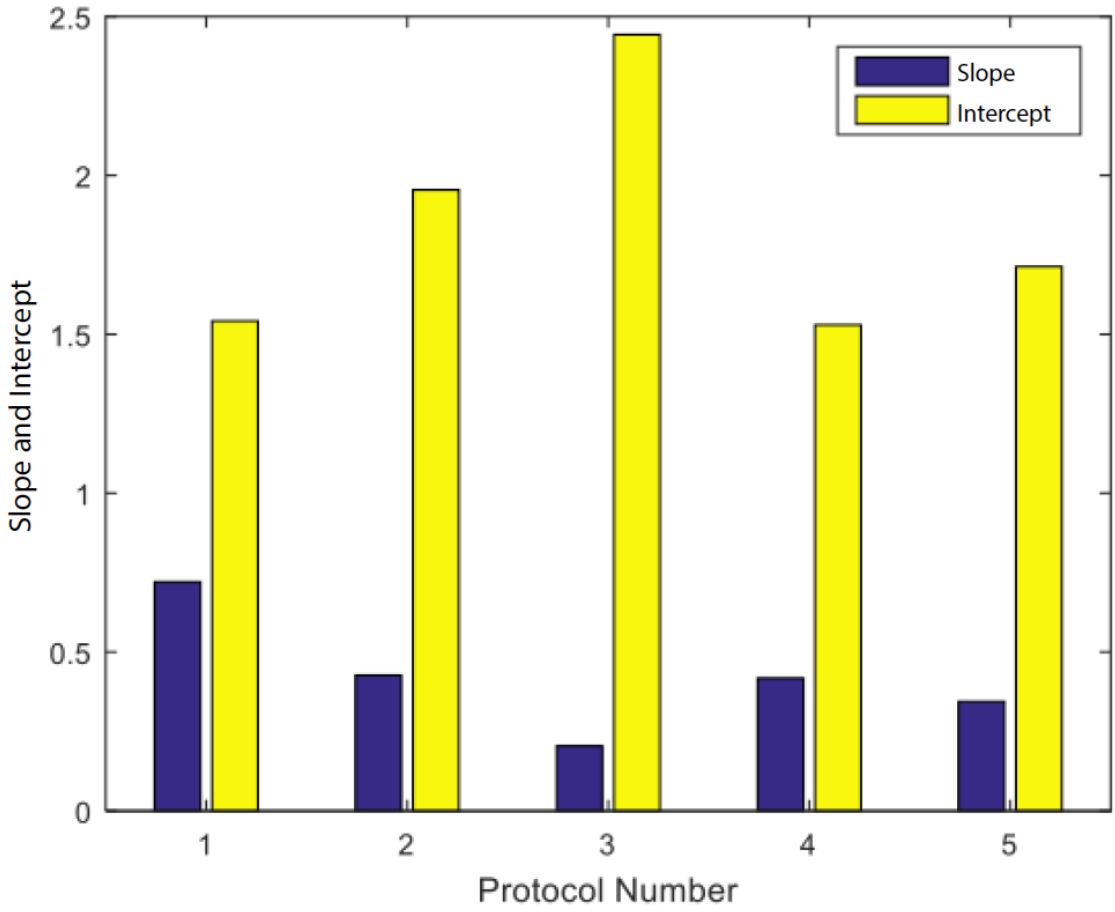

Figure 3.4: Slope and intercept of a linear fit on pursuer speed vs. evader speed. The speeds are better matched when the slope is closer to one and the intercept is closer to zero. This information is also presented in Table 3.1.

3.2 Analysis of Proportional Navigation

If we imagine that the pursuer is performing a proportional navigation strategy (as mentioned in chapter 1.4.2), the constant *N* can be computed. In this case, the pure proportional navigation (PPN), true proportional navigation (TPN) and ideal proportional navigation strategies are explored using equation 1. Fitting the data to equation 1, we find that the fit equation explains

very little or none of the variances in the data (R-squared values < 10^{-2}). See Table 3.2. Thus, the concept of proportional navigation is not likely to be explanatory of pursuer dynamics. The poor fit may also be because of the noisy acceleration values needed for this analysis.

Table 3.2: R^2 values for Proportion Navigation

	Protocol 1	Protocol 2	Protocol 3	Protocol 4	Protocol 5
N (PPN)	1.4×10^{-4}	3.4×10^{-4}	1.5×10^{-4}	4.8×10^{-5}	1.8×10^{-4}
N (TPN)	1.3×10^{-4}	5.3×10^{-4}	5.8×10^{-5}	8.9×10^{-7}	1.5×10^{-4}
N (IPN)	5.3×10^{-5}	5.8×10^{-5}	5.6×10^{-4}	1.1×10^{-3}	6.4×10^{-4}

3.3 Step-up Linear Regression of Pursuer Motion

In this section, we try to construct a model to predict the pursuer's speed (V_p) and relative heading (θ_{PE}) using the other parameters that we collected or interpreted from the experiment, which are also available to the pursuer. Let the speed of the pursuer be a sum of the combination of the following parameters: evader speed (V_e); evader relative heading (β); the relative distance between pursuer-evader (PE); shortest distance from pursuer position to the room boundary (d_{P2B}); shortest distance from evader position to boundary (d_{E2B}); mass of pursuer (m_P) and evader (m_E). See figure 3.5. The acceleration data that can be obtained by differentiating the velocity data was found to be too noisy for analysis.

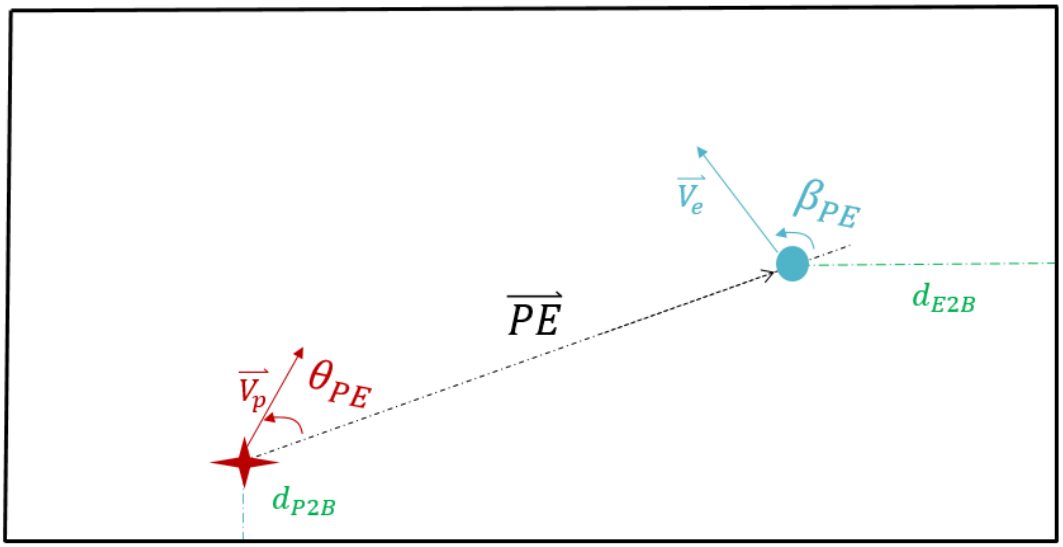

Figure 3.5: Visualization of modeling parameters

Model 1:

For our first model, we hypothesized that the pursuers speed (V_p) is a linear function of the evader's speed and the relative distance between the pursuer and the evader. That is,

$$V_p = \lambda_1 V_e + \lambda_2 PE + \lambda_3$$

where $\lambda_1, \lambda_2 and\ \lambda_3$ are proportionally constant. Using the data collected from the experiment, the values of λ_1, λ_2 and λ_3 are calculated for each protocol, using the function "fitlm" in MATLAB. The significance of each constant is evaluated using criteria that the p-value must be less than 0.05. The overall fit of the model to the data is expressed using its corresponding R^2 value. Look at Table 3.3 for the computed values.

Table 3.3: Model 1 – Calculated Parameters and Significance

	λ_1 (Significant)	λ_2 (Significant)	λ_3 (Significant)	R^2 value
Protocol 1	0.742 (Yes)	-0.063 (Yes)	1.724 (Yes)	0.661
Protocol 2	0.442 (Yes)	-0.059 (Yes)	2.109 (Yes)	0.344
Protocol 3	0.1588 (Yes)	-0.034 (Yes)	2.751 (Yes)	0.074
Protocol 4	0.400 (Yes)	-0.041 (Yes)	1.704 (Yes)	0.411
Protocol 5	0.310 (Yes)	-0.081 (Yes)	2.041 (Yes)	0.291

For Table 3.3, we can see that this simple model best predicts the pursuer speed in protocol 1 and poorly predicts it in protocol 3. Though only two parameters are used without any normalization for different pursuer-evader property (e.g., mass), model 1 seems reasonably predictive for human pursuer velocities. We also see that the less the evader is constrained, the less predictable his/ her motion is to the pursuer as implied by the decreasing R^2 value as constraints on the evader are decreased.

Model 2:

When the square of distance between pursuer and evader (PE) is added i.e. PE^2, the resulting model 2,

$$V_p = \lambda_1 V_e + \lambda_2 PE + \lambda_3 PE^2 + \lambda_4,$$

performs significantly better in the free form case (protocol 3's R^2 goes to about 0.4 from less than 0.1), while slightly improving the R^2 value in the other cases. Look at Table 3.4.

Table 3.4: Model 2 – Calculated Parameters and Significance

	λ_1 (Sgfnt)	λ_2 (Sgfnt)	λ_3 (Sgfnt)	λ_4 (Sgfnt)	R^2 value
Protocol 1	0.738 (Yes)	-0.0009 (Yes)	-0.0079 (Yes)	1.637 (Yes)	0.661
Protocol 2	0.447 (Yes)	0.259 (Yes)	-0.041 (Yes)	1.645 (Yes)	0.358
Protocol 3	0.117 (Yes)	0.505 (Yes)	-0.039 (Yes)	1.646 (Yes)	0.387
Protocol 4	0.397 (Yes)	0.078 (Yes)	-0.017 (Yes)	1.538 (Yes)	0.413
Protocol 5	0.311 (Yes)	-0.055 (Yes)	-0.019 (Yes)	1.839 (Yes)	0.294

Model 3:

In model 3, we add linear terms corresponding to distances of the pursuer (d_{P2B}) and evader (d_{E2B}) to the defined boundaries of the room. That is,

$$V_p = \lambda_1 V_e + \lambda_2 PE + \lambda_3 PE^2 + \lambda_4 d_{E2B} + \lambda_5 d_{P2B} + \lambda_6$$

We found that evader distance to boundary was less significant in protocol 1 and 2 than the pursuer distance to the boundary. This was surprising since it was hypothesized that the both the pursuer and evaders distance to the boundary would be significant. Further, these extra terms only slightly improved the model. See Table 3.5.

Table 3.5: Parameters Significance and R^2 values of model 3

	d_{E2B} SGFNT	d_{P2B} SGFNT	R^2 value
Protocol 1	No	Yes	0.701
Protocol 2	No	Yes	0.367
Protocol 3	Yes	Yes	0.315
Protocol 4	Yes	Yes	0.425
Protocol 5	Yes	Yes	0.311

Model 4:

After trying numerous combinations of different parameter in both linear and non-linear combinations, we used "symbolic regression" from a genetic programming toolbox in Matlab to find the best fit (Searson 2015). For this regression, we only used our initial variables (V_e, PE) to model V_p. The following is model is the best fit when all data is used:

$$V_p = \lambda_1 V_e - \lambda_2 V_e^2 (PE + \lambda_3) + \lambda_4 PE^3 (V_e + PE) - \lambda_5 PE^2 - \lambda_6 (PE - \lambda_7)^2 + \lambda_8 V_e (V_e + \lambda_9)(V_e - PE) - \lambda_{10} PE^2 (V_e + PE)^2 (PE - \lambda_{11})(PE - \lambda_{12})(PE^2 - PE + V_e) + \lambda_{13}$$

Table 3.6: Model 4 –Significance

	R^2 value (model 2)	R^2 value (model 4)	Difference in R^2
Protocol 1	0.661	0.666	0.005
Protocol 2	0.358	0.385	0.027
Protocol 3	0.387	0.437	0.050
Protocol 4	0.413	0.422	0.009
Protocol 5	0.294	0.323	0.029

The significance of this model 4 is that it can more accurately predict the pursuer velocity. But compared to model 2 and the additional level of complexity it introduces, this model didn't improve the model more accurately than model 2. See Table 3.6.

Model 5:

Analogous to the models above, we obtained the best-fit model to represent the relative heading (θ_{PE}) as well. The simplest model is similar to model 1 is also implement, i.e. (θ_{PE}) being a linear sum of pursuer-evader distance (PE) and speed of evader (V_e).

$$\theta_{PE} = \lambda_1 V_e + \lambda_2 PE + \lambda_3$$

We see in Table 3.7 that this model does quite poorly in explaining the relative heading (low R^2 values). But both evader speed and pursuer-evader distance were found to be significant.

Model 6:

Here we try to see the effects of the evader angle (β) with respect to the pursuer evader vector (PE) in predicting the relative pursuer angle. Model 6 includes all the variables in model 5 and adds another term linearly to represent the relative evader angle (β). That is,

$$\theta_{PE} = \lambda_1 V_e + \lambda_2 PE + \lambda_3 \beta + \lambda_4$$

We see in Table 3.7 that this model improved the model accuracy significantly.

Model 7:

Using the symbolic regression (Searson 2015) on all the data we obtain the following model 7.

$$\theta_{PE} = \lambda_1 V_e + \lambda_2 PE + \lambda_3 \beta + \lambda_4 \beta^2 + \lambda_5 \beta^3 + \lambda_6 V_e \beta + \lambda_7 \beta PE +$$

$$\lambda_8 (V_e - \beta)(PE + 2\beta)(V_e + 2\beta - \beta(V_e - \beta)) + \lambda_9$$

Table 3.7: Model 5, 6 and Model 7 significance

	R^2 value (Model 5)	R^2 value (Model 6)	R^2 value (Model 7)	Difference in R^2 between Model 6 and 7
Protocol 1	0.045	0.350	0.506	0.156
Protocol 2	0.142	0.326	0.454	0.128
Protocol 3	0.109	0.382	0.494	0.112
Protocol 4	0.194	0.572	0.631	0.059
Protocol 5	0.114	0.502	0.548	0.046

From Table 3.7, the non-linear complexity introduced in this model seems to have increased the model accuracy, since the complex model increased the R^2 value beyond that of the simpler model 6. To avoid over-fitting, we test the generalizability of this model by inferring it from only half the data and testing its predictive ability on the other half of the data.

3.4 Discussion

3.4.1 Qualitative Assessment of Subject Behavior

We now describe some qualitative characteristics that subjects exhibited during the trials that we did not support quantitatively with data. For instance, the evader tended to not always change directions, even when it could have been beneficial to change directions, like protocol 2 and 5. We might speculate that this behavior could indicate that either a behavior dislike to change direction or a biological incapability (or energetically expensive) to change directions. We informally observed that the evader would sometimes repeat the same kind of evasion patterns that they used in a previous trial. Perhaps this was because the evader did not consider this a real game, as opposed to an experiment.

Pursuer, in general, seems to be using some kind of lead strategy when the evader is more predictable (more constrained). When the evader is less constrained and therefore less predictable, the pursuer seems to implement some kind of lag or pure strategy. The implementation of the strategy seems asymmetric, so that when the pursuer performs lead-strategy, he/she would lead up to 30^0, whereas when a lag-strategy is performed, he/she would only lag up to 3^0 (which may be within our angle estimation accuracies). While the median show lead or lag, the standard deviations are quite large compared to the median, so that they may not exactly pure, lead, or lag in any single trial, just on average.

3.4.2 Possible Sources of Error or Complexity in the Experiment

The boundary of the rooms may have placed some unintended constraint in the experiment. It is observed (mainly in protocol 1 and 2) that the evader would sometimes sprint to the end of the

room and wait for the pursuer, rather than actually performing an evasive strategy. Any suggestion from the experimenter to avoid this strategy can bias the strategy used by the evader, so we did not instruct the evader to explicitly avoid such simple movement strategies. One potential solution to this problem is to make the room (or field) much bigger, so that capture can happen before they can reach the boundary. This will avoid boundary effects in the strategies used.

While the trials do impose considerable levels of exertion on the subjects, subject fatigue in this experiment was likely not significant because the subjects were allowed to take long breaks upon request in between trails. Also, though the pursuers were instructed to catch the evader as soon as possible, the subjects didn't perform the best version of pursuit, for instance, often using lower than their maximum speeds. It is possible that effectiveness of our instructions wears off on the subject with each passing trial, thus causing them to not perform at their best.

The camera-based motion measurement system has small errors due to the resolution of the measuring device, object calibration error, reference location identification error, camera calibration matrix error, cap identification error, and 3-D position reconstruction error. These errors in computing pursuer and evader 3-D coordinate can be considered not significant since it's within $\pm$ 0.2m. This error, compared to the overall room perimeter (36m), is an error of only 0.55%. These positions errors lead to relatively small velocity errors because they are systematic rather than random. Also, since we are mainly interested in the overall trends, such errors may not matter as much for the qualitative conclusions drawn.

Chapter 4: Conclusion and Future Work

In conclusion, we have experimentally characterized the strategies used by humans in pursuing an evading target and compared our experimental data with a few simple pursuit strategies. During pursuit, humans use a combination of pure, lead and lag strategy to catch an evading target. The degree of this lead or lag pursuit versus pure pursuit seems based on how constrained or predictable the evader's motion is. We fit multiple mathematical models for pursuer speed to experimental data. We found that a simple model that depended linearly on evader speed and quadratic on the pursuer-evader distance explained at worst 29% and at best 66% of the variance in the pursuer speed, depending on evader motion (straight line versus free form). We also found that modeling the angle between pursuer and line PE (between pursuer and evader) using a simple model that depended linearly on evader speed, pursuer-evader distance and relative evader angle explained at worst 33% and at best 57% of the variance in this angle, depending on evader motion constraints. This angle variance was on average 10% better explained introducing the non-linear model using symbolic regression. Thus with our current models, we can explain 40% of pursuer motion in free form (39% of pursuer speed variance and 38% of pursuer angle variance). The 'complex' models that we obtained using symbolic regression (Models 4 and 7) were mainly exploratory in nature. We do not associate any biological significance to them at this point, as they appear to be too complex to be interpretable.

Most models we have considered are quite simple and have not yet included some variables that might improve predictability of pursuer motion. Instead of characterizing pursuer velocity as "magnitude and angle", we could test if linear models can better predict the pursuer velocity along and perpendicular to PE. Analogously, explanatory variables in such linear models could

use be evader speed along and perpendicular to PE, the distance PE, and the distance to the boundary. We could also use smoothed acceleration of the evader as a predictor, although this variable is not very reliable because of differentiation errors. Such unreliable acceleration may partly be responsible for poor performance of proportional navigation models, as they rely on acceleration information.

Ongoing and future work will involve testing of potentially more complex models with more explanatory variables as detailed above. We have not yet used information regarding body orientation available through the IMU's on our pursuers and evaders, and such information may lead to improved predictive models. Body orientation is an important determinant of running speed, as humans can run much faster sideways than forward, and cannot change direction instantaneously. More detailed marker-based motion capture may also provide further information about movement strategies. A related aspect to explore would be the role of head orientation and the use of central versus peripheral vision in pursuit and evasion. In this thesis, we have focused on pursuer motion as a function of evader motion. But at least in the protocol with free-form evader motion, we could try to examine the data to obtain simple evasion strategies as a function of pursuer motion.

In future experiments, we hope to repeat the protocol with free-form evader motion in a much larger field – large enough that boundary effects are ignorable and the boundary is never reached. To better control the evader movement, we could use a precisely programmed wheeled robot (or even one of the researchers) instead of a human subject. Future experiments can also add more than one evader or pursuer to learn the dynamics used by people when multiple pursuers or

evaders are present. We also like to study the pursuit strategies used, when the pursuer is slower than the evader. Further, we also like to see if there is any difference in results when a trained subject (experienced played) performs the experiments vs. the untrained subjects (like in this experiment). We speculate that the R^2 values in the model would increase with respect to its untrained counterpart, due to higher coordination and prior practice.

In conclusion, we have taken the experimentally characterize human pursuit in pursuit-evasion games, and compared this data with simple models, laying a strong foundation for more detailed analysis in future work.

Bibliography

[1] R. McN. Alexander. *Mechanics of bipedal locomotion*, In: *Perspectives in Experimental Biology*, volume 1, 493-504, Pergamon Press, New York, 1976.

[2] R. McN. Alexander. *Optimization and gaits in the locomotion of vertebrates*, *Physiological Review*, 69, 1199-1227, 1989.

[3] R. McN. Alexander. *Principles of Animal Locomotion*, Princeton University Press, Princeton, 2003.

[4] J. Connell. *Pursuit and Evasion Strategies in Football*. The Physics Teacher, 33, 516-518, 1995.

[5] D. Ghose. *An introduction to proportional navigation*. National Programme on Technology Enhanced Learning, online, Lecture 22 in Guidance of missiles, 2012.

[6] D. F. Hoyt and C. R.Taylor. *Gait and the energetics of locomotion in horses*, *Nature*, 292, 239-240, 1981.

[7] L. Long III and M. Srinivasan. *Walking, running and resting under time, distance, and speed constraints: Optimality of walk-run-rest mixtures*. *Journal of Royal Society Interface*, 10, 20120980, 2013.

[8] E. Lynch. *Tactics 101 – Introduction and lag pursuit.* SimHQ, online, 1998.

[9] E. Lynch. *Tactics 101 –Pure and lead pursuit.* SimHQ, online, 1998.

[10] P. J. Nahin. *Chases and escapes: The mathematics of pursuit and evasion.* Princeton University Press, Princeton, 2012.

[11] N. F. Palumbo, R. A. Blauwkamp and J. M. Lloyd. *Basic principles of homing guidance*. Johns Hopkins APL Technical Digest, 29, 25-41, 2010.

[12] H. J. Ralston. *Energy-speed relation and optimal speed during level walking.* Int. Z. Angew. Physiol. 17, 277-283, 1958.

[13] D. Searson, *DP. GPTIPS 2: an open-source software platform for symbolic data mining*. Chapter 22 in Handbook of Genetic Programming Applications, A.H. Gandomi et al., (Eds.), Springer**,** New York, NY, 2015.

[14] M. Srinivasan. *Optimal speeds for walking and running, and walking on a moving walkway. CHAOS*, 19, 026112, 2009.

Appendix A: Data Processing using Multiple cameras

Three cameras are used to capture the dynamics of the pursuer-evader motion. Both the pursuer and evader are wearing two different colored hats to be easily identified in the camera image. The 3-D coordinates of fourteen unique points in the environment were collected during the experiment to calibrate the cameras. Each of the cameras was individually characterized with ten different camera specific properties. The ten different properties are rotational angles (with respect to all three planes), its 3D translations, its focus and scaling on the image (2 corresponding components) and a 2-D offset in the image (2 components). Using the calibration data collected during the experiment, this ten camera parameter set was calculated and correctly calibrated using the optimization of the prediction error. We used fsolve() function in Matlab combined with multiple user defined function to calculate these parameters.

World2Image.m is one of the three user defined function needed to calibrate the camera matrix. This function transforms the 3D world coordinates to camera coordinates.

```
function pointImage = World2Image(pointWorld,pinput)
    theta1 = pinput(1);%rotational angles
    theta2 = pinput(2);
    theta3 = pinput(3);
    x0 = pinput(4);%3-D camera translation
    y0 = pinput(5);
    z0 = pinput(6);
    f1 = pinput(7);%focus + scaling on image
    f2 = pinput(8);
    u0 = pinput(9);%2D origin offset on image
    v0 = pinput(10);

    Rx = [1 0 0; ...
        0 cos(theta1) -sin(theta1);
        0 sin(theta1) cos(theta1)];
    Ry = [cos(theta2) 0 sin(theta2);
        0           1    0;
        -sin(theta2) 0   cos(theta2)];
    Rz = [cos(theta3) -sin(theta3) 0;
        sin(theta3) cos(theta3) 0;
        0 0 1];
```

```
    %rotation matrix
    RotMat = Rx*Ry*Rz;

    % transform to a 3D frame fixed to camera
    pointCamera = RotMat*pointWorld + [x0; y0; z0];

    % perpective projection
    u_Camera = f1*pointCamera(1)/pointCamera(3)+u0;
    v_Camera = f2*pointCamera(2)/pointCamera(3)+v0;

    pointImage = [u_Camera; v_Camera];

end
```

Once the camera parameters are found, the pursuer/ evader location on the three camera frames (2-D images) can be used to reconstruct the [x y z] points of the pursuer/ evader in the world coordinates. Mathematically, at least two cameras with 10 calibration points are needed to reconstruct the 3-D matrix of the pursuer/evader. We used more calibration points to add redundancy to more accurately model the camera matrix and get more accurate pursuer-evader positions.

Here is our 3-D reconstruction code, assuming that you know the [x y] position of the intended marker on camera plane and the camera calibration matrix.

```
function Wpoint =
CamView2World_3cam(camclick1,camclick2,camclick3,CamPar1,CamPar2,CamPar3,oldp
oint)
      for i = 1:10 % solve it 10 time, as it uses ensures that different part
%     %of the non-linear Typology is explored to a global min (lowest error)

        Wx0 = 300*rand(1,1); %x initial seed
        Wy0 = 500*rand(1,1); %y initial seed
        Wz0 = 70*rand(1,1);  %z initial seed
        Wpoint0 = [Wx0;Wy0;Wz0];

        options = optimset('display','iter'); % accuracy/convergence

      [Wpointemp(i,:),error] =
      fsolve(@fResidual,Wpoint0,options,camclick1,camclick2,camclick3,CamPar1
      ,CamPar2,CamPar3);
        Error1_cam(i) = max(abs(error));
        Error2_cam(i) = min(abs(oldpoint-Wpointemp(i,2)));
        Error3_cam(i) = Error2_cam(i) < 200;
```

```
    end
    [~,MinIndex] = min(Error1_cam);
    [~,MinIndex2] = min(Error2_cam);


    Wpoint = Wpointemp(MinIndex,:);

    if Error1_cam(MinIndex) > 0.9*Error2_cam(MinIndex2)
        Wpoint = Wpointemp(MinIndex2,:);
    end

    if camclick1(1) ==0 && camclick3(2) == 0
        Wpoint = [nan; nan; nan];
    end
end

%%
function f =
fResidual(Wpoint0,camclick1,camclick2,camclick3,CamPar1,CamPar2,CamPar3)

    pointImage1 = World2Image(Wpoint0,CamPar1);
    pointImage2 = World2Image(Wpoint0,CamPar2);
    pointImage3 = World2Image(Wpoint0,CamPar3);

    f1 = pointImage1-camclick1;
    f2 = pointImage2-camclick2;
    f3 = pointImage3-camclick3;

    if camclick1(1) ==0 && camclick3(2) == 0
        f = [0;f2;0];
    elseif camclick1(1) ==0 && camclick1(2) == 0
            f = [0;f2;f3];
    elseif camclick2(1) ==0 && camclick2(2) == 0
            f = [f1;0;f3];
    elseif camclick3(1) ==0 && camclick3(2) == 0
            f = [f1;f2;0];
    else
        f = [f1;f2;f3];
    end

end
```

One drawback in using an optics based sensing is that the light condition in the room can drastically change the final answers. Further, interference between the camera and the sensed object because an issue of manually clicking the camera images. Some of the experiments in our case were conducted mid-day and the lighting was so bad that we couldn't even see the person properly, let alone see the marker hat. So we ignored such data sets too difficult to process.